

# Application of Polyimide-based Microfluidic Devices on Acid-catalyzed Hydrolysis of Dimethoxypropane

Jens Bobers\*, Elisabeth Forys, Bastian Oldach, and Norbert Kockmann

DOI: 10.1002/cite.202000224

 This is an open access article under the terms of the Creative Commons Attribution License, which permits use, distribution and reproduction in any medium, provided the original work is properly cited.

Microfluidic devices intensify transport phenomena and can improve chemical processes. New manufacturing processes and materials are perpetually developed due to constantly growing interest in process intensification. In this contribution, the authors present the design and application of polyimide-foil-based microfluidic mixing devices manufactured by reactive ion etching. As appropriate model reaction system, acid-catalyzed 2,2-dimethoxypropane (DMP) hydrolysis was chosen and investigated in three different mixing structure with varying flow rate. Energy dissipation rates were calculated to estimate mixing performances. The results show good mixing quality for Reynolds numbers between 10 and 100 and similar mixing times scales for all investigated microstructured mixers.

**Keywords:** Acid-catalyzed hydrolysis, Microreactor, Mixing, Polyimide foil

*Received:* October 26, 2020; *revised:* January 12, 2021; *accepted:* February 05, 2021

## 1 Introduction

With steadily growing interest and development in modern chemistry, life science, and pharmaceutical manufacture, research as well as industry have to face challenges, which cannot be treated by using conventionally sized plants. Microfluidic applications adapt necessary requirements to overcome limits set by the dimensions of macroscopic devices and led to a growing field of research in recent years [1]. These applications are used to perform reactions rather in continuously operated processes instead of conventional batch [2].

Enhanced performance parameters such as heat and mass transfer rates lead to higher efficiencies, also known as process intensification in miniaturized equipment. These improved transport rates feature purposes such as rapid mixing or facilitated temperature control of highly exothermic reactions [3]. Since diffusive mass transfer is the key parameter within microfluidic applications, micromixers are designed in a way that diffusive transport length scales are minimized. This is achieved when convective mass transport is induced and the surface boundary layer between reactants is enlarged. Especially fast reactions benefit from rapid mixing and improved heat transfer. Hence, there is a need to overcome limitations set by prevailing laminar flow. Microscopic-scaled devices show improved mixing efficiency compared to macroscopic mixers. In addition, passive micromixers stand out through low fabrication costs, easy integration into microfluidic systems, and

without any need of complex process control units or additional energy input [4].

As a result of industrial development, microfluidic applications become increasingly important, so that new and improved manufacturing processes and designs for microreactors or other microfluidic systems must be constantly improved. For the development of new microfluidic devices, the material selection is of decisive importance. Polyimide (PI) is classified as a high-performance polymer due to its properties and so far, it has been used in electronics, aeronautics, and space technology. Due to its thermal stability and resistance to solvents as well as acids and bases, it is ideally suited for chemical applications, too [5].

Flexibility, low cost, and reproducibility are the main requirements, which should be met by a manufacturing process for microfluidic devices suitable for different applications. Thin-film technology is employed in thin-film deposition processes, a technology that is applied in many large-scale electronic applications such as mass production of transistors, actuators, and sensors. Reactive ion etching provides a high anisotropic etching behavior and an adjustable etching mechanism since the gas composition used for

---

Jens Bobers, Elisabeth Forys, Bastian Oldach,  
Prof. Dr.-Ing. Norbert Kockmann  
jens.bobers@tu-dortmund.de  
TU Dortmund University, Department of Biochemical and  
Chemical Engineering, Emil-Figge-Straße 68, 44227 Dortmund,  
Germany.

etching can be varied during the fabrication steps. The combination of both processes is evaluated in this contribution as a manufacturing process for PI-based microstructured devices characterized by a high spatial resolution and a highly anisotropic etching mechanism suitable to produce rectangular microchannels.

Applying beforehand optimized process parameters [6], three micromixing structures were manufactured. To gain deeper insight into the mixing efficiency of each produced microstructure, a consecutive and competitive reaction scheme as the acid-catalyzed hydrolysis of 2,2-dimethoxypropane (DMP) with the neutralization of hydrochloric acid with sodium hydroxide allows statements about the mixing behavior inside the structure. Rinke et al. [7] and Schwolow et al. [8] investigated this parallel reaction to obtain information about mixing performance inside several microreactors.

Evaluation of the mixing performance of each micromixer is carried out using an online UV/Vis spectroscopy for reaction monitoring and subsequent calculation of the yield of the reaction regarding acetone.

## 2 Design of Mixing Structures

The investigated microstructures are designed in a way to achieve efficient mixing of aqueous single-phase flows as well as multiphase flows. Literature provides various geometries to generate mixing within different microscopic scaled applications. [9]

### 2.1 Tangential Mixer

The designed tangential mixer consists of totally 14 mixing chambers arranged in series. They are connected by constriction channels featuring a width of 200  $\mu\text{m}$ , which are tangentially aligned to smoothly introduce the fluid into the mixing chamber creating self-circulation. Within these constrictions, the fluid is accelerated and the distance for diffusive mass transfer is reduced. The ratio of the diameter of the circulation chamber to the width of the constriction as a crucial design parameter was set to 4.1 according to the tangential mixers designed by Ansari and Kim [10] and led to a diameter of the circulation chamber of 800  $\mu\text{m}$ . The distance between consecutive mixing chambers is 1 mm.

### 2.2 Dean Mixer

The investigated Dean mixer consists of 15 loops. They feature a consistent channel diameter of 200  $\mu\text{m}$  over the whole mixing length. The circumference of each loop is  $5\pi/6$ , which results in an opening angle of 60°. The inner radius of

the loops is 567  $\mu\text{m}$ ; consequently, the outer radius is 767  $\mu\text{m}$ . The distance between two consecutive loops on the same symmetry axis is 1.6 mm. The dimensions were determined based on the investigations of Ugaz et al. [11] and Schönefeld et al. [12].

### 2.3 SZ Mixer

SZ mixers are common micromixing structure with a variety of applications [13] and consist of four alternating S and Z shaped loops. Each S element is connected to a Z element by an 800  $\mu\text{m}$  long and 200  $\mu\text{m}$  wide straight channel and the other way around. In a direct transition from one curve to the next, the channels are narrowed to 120  $\mu\text{m}$  in widths. This constriction enhances diffusive mixing due to shorter diffusion length and accelerates the fluid. The geometry was created according to Tollkötter et al. [14].

### 2.4 Manufacturing Process

The manufacturing process is divided into two main parts. First, for creating a hard mask from aluminum on the PI foil, the PI substrate is cut und cleaned. Photoresist is spun onto the surface of the substrate by spin coating. After baking, the resist is exposed to UV light and developed to create a negative of the wanted mask structure. To gain the positive mask, the PI foil is covered with aluminum by high-frequency cathodic sputtering. Unwanted aluminum is removed by lift-off with acetone. Subsequently, reactive ion etching is used as a bulk structuring strategy to generate the desired microchannels within the PI foil. [6]

## 3 Experimental Setup

The experimental setup as shown in Fig. 1 consists of two syringe pumps (VIT-FiT, Lambda Instruments GmbH, Barr, Switzerland) with 50-mL syringes (Henke-Ject, Henke-Sass Wolf GmbH, Stuttgart, Germany) and a thermostat (Polystat cc2, Peter Huber Kältemaschinenbau GmbH, Offenburg, Germany), in which the two feeds are preheated to 25 °C.

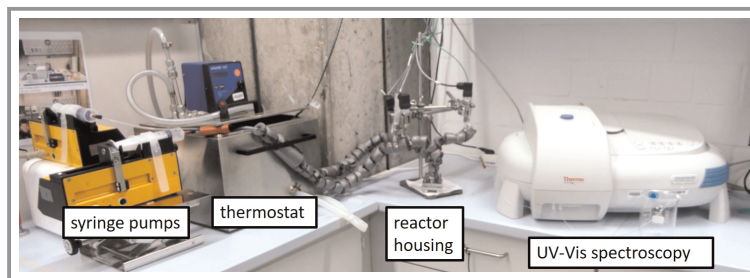


**Figure 1.** Experimental setup including syringe pumps, preheated feed streams, housed microfluidic device connected to pressure and temperature sensors, and UV/Vis spectrometer for online analysis.

Insulated tubes connect the pumps to the microreactor. Fig. 2 presents the in-house custom-made mixing structures manufactured by reactive ion etching. Here, Kapton<sup>®</sup> HN (E. I. du Pont de Nemours and Company, Wilmington, USA) with a thickness of 125  $\mu\text{m}$  was utilized as substrate.

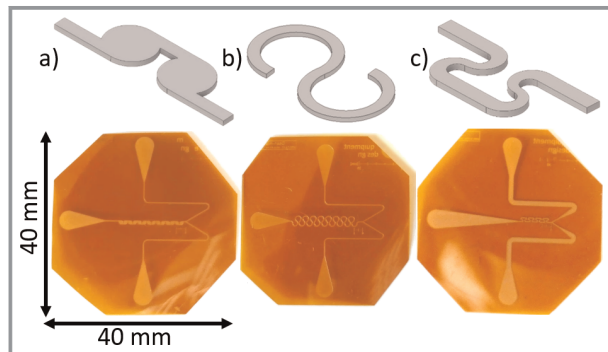


**Figure 2.** Schematics of the investigated PI-based micromixing structures (top) and corresponding pictures of the manufactured planar polyimide-based microreactors with inlets and outlet (bottom): a) tangential mixer, b) Dean mixer, c) SZ mixer.

All tubes are connected via Hy-Lok compression fittings (Hy-Lok D Vertriebs GmbH, Germany). A reactor housing links the tubing with the PI-based mixing structures [6].

Tab.1 demonstrates characteristic data for all investigated mixing structures at a volumetric flow rate of  $1.635 \text{ mL min}^{-1}$ , which corresponds to the highest possible pressure drop of 2.5 bar in the Dean 1 mixer.

For evaluation of reaction progress and mixing quality, sensory for temperature (IKF 05/10, ES Electronic Sensor GmbH, Heilbronn, Germany) and pressure (WIKA Alexander Wiegand SE & Co. KG, Klingenberg, Germany) is installed at both inlets and the outlet. The data obtained is supplied to a LabVIEW (National Instruments Germany GmbH, Munich, Germany) interface monitoring and storing measured signals. An UV/Vis spectrometer (Thermo Scientific Evolution 201 spectrometer, Schwerte, Germany) delivers online concentration measurements with a measurement interval of 0.1 s. A confocal laser-scanning microscope (VK-X 100, Keyence, Neu-Isenburg, Germany) enabled the evaluation of the quality of the etched surface and was used to determine the root mean square roughness as shown in Tab.1. The difference of properties between Dean 1 and Dean 2 mixers results from a higher etching depth for Dean 2 mixer. For both channels the width is identical with  $200 \mu\text{m}$  but the etching depths are 95 and  $113 \mu\text{m}$ , respectively.

The reaction scheme of the acid-catalyzed DMP hydrolysis as well as the competitive neutralization reaction are shown in Fig. 3a. Fig. 3b displays feed compositions accor-

**Table 1.** Characteristic data for tangential, SZ, and both Dean mixers at a volumetric flow rate of  $1.635 \text{ mL min}^{-1}$  including hydraulic diameter and surface roughness of the etched channel.

Mixer type	Mixing volume $V_{\text{mix}}$ [ $\mu\text{L}$ ]	Hydraulic residence time $\bar{\tau}$ [ms]	Aspect ratio $a$ [-]	Reynolds number $Re$ [-]	Root mean square roughness $R_q$ [ $\mu\text{m}$ ]	Hydraulic diameter $d_h$ [ $\mu\text{m}$ ]
Tangential	0.948	3.5	0.501	181.6	$2.1 \pm 0.6$	134.1
Dean 1	1.085	4.0	0.464	186.2	$1.7 \pm 0.3$	127.2
Dean 2	1.288	4.7	0.550	175.8	$4.0 \pm 2.0$	141.1
SZ	0.306	1.1	0.864	243.7	$3.0 \pm 2.0$	110.3

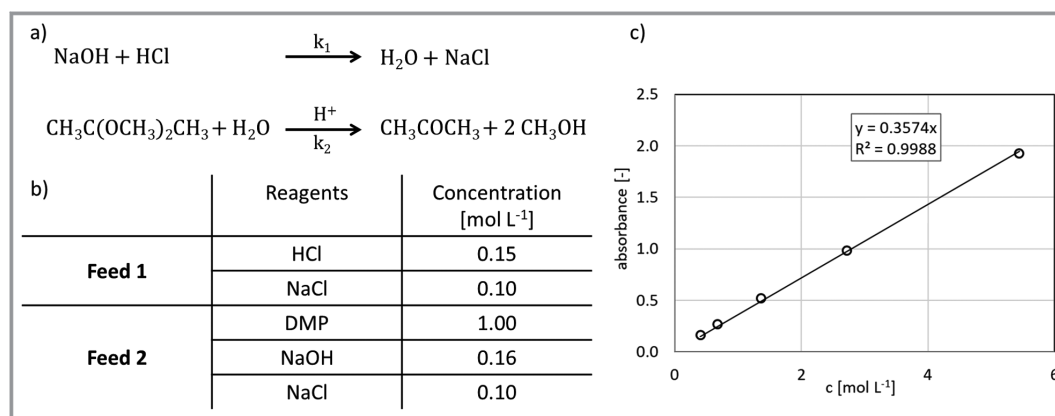


**Figure 3.** a) Fast neutralization and slower acid-catalyzed DMP hydrolysis as competitive reaction system. b) Reagents and feed compositions according to Rinke et al. [7]; 25 wt % ethanol in water as solvent for both feeds. c) Calibration curve for acetone in 25 wt % ethanol-water mixture and  $0.1 \text{ mol L}^{-1}$  NaCl measured by UV/Vis spectroscopy at a wavelength of 271 nm.

ding to Rinke et al. [7]. UV/Vis measurement of acetone was calibrated in actual solvent mixture as it is used in the feed including  $0.1 \text{ mol L}^{-1}$  NaCl. The resulting calibration line at a wavelength of 271 nm is shown in Fig. 3c.

## 4 Results and Discussion

Evaluating the mixing quality of the microstructures, the volumetric flowrates and, thus, the Reynolds number were varied, and the obtained yields of acetone measured via UV/Vis spectroscopy are presented in Fig. 4. As expected, the yield decreases with increased volumetric flow rate and Reynolds number. For Reynolds numbers higher than 40, all mixing structure reveal acetone yields below 1%. For higher Reynolds numbers a further decreasing of the yield could not be observed.

For Reynolds numbers lower than 35, the obtained yields for the tangential mixer decrease moderately from 2.2 % to about 1 %. Both Dean mixers behave differently as the yields for Dean 1 falling from 3.3 % to 1 % but the yield obtained with the Dean 2 reduces from 2.2 % down to 0.7 %. The SZ mixer shows the highest yields between 3.5 % and 5.2 %. For better comparison of the data, the obtained yields are plotted against the measured pressure loss over the mixing length; as shown in Fig. 4b.

For a pressure drop higher than 0.6 bar, the tangential mixer, the Dean 2 mixer, and the SZ mixer show comparable mixing quality. The SZ mixer leads to lowest acetone yields for high pressure losses, as shown in Fig. 4b. For lower pressure drops and therefore lower flow rates, the mixing performances decreases. Assumingly, in the SZ mixer secondary flow patterns are only introduced at higher Reynolds numbers, which accelerates the mixing. The overall highest pressure drop measurements were observed for the Dean 1 mixer. For further comparison and evaluation of the mixing time scale, the specific energy dissipation rate is calculated as shown in Holvey et al. [13].

$$\varepsilon = \frac{\dot{V}\Delta p}{V} \quad (1)$$

The energy dissipation rate is derived in accordance with Eq. (1) from the pressure drop  $\Delta p$ , the volumetric flow rate  $\dot{V}$ , and the mixing volume  $V$ , which is responsible for the measured pressure drop. The acetone yield is plotted logarithmically against the energy dissipation rate in Fig. 4d. The plots are linearized, where the similar relation of energy dissipation rate and yield of acetone can be observed for all mixing structures. A power law regression was fitted to the experimental data obtaining an exponent  $n = -0.56$ , which is close the theoretical value of  $-0.5$  [15–17].

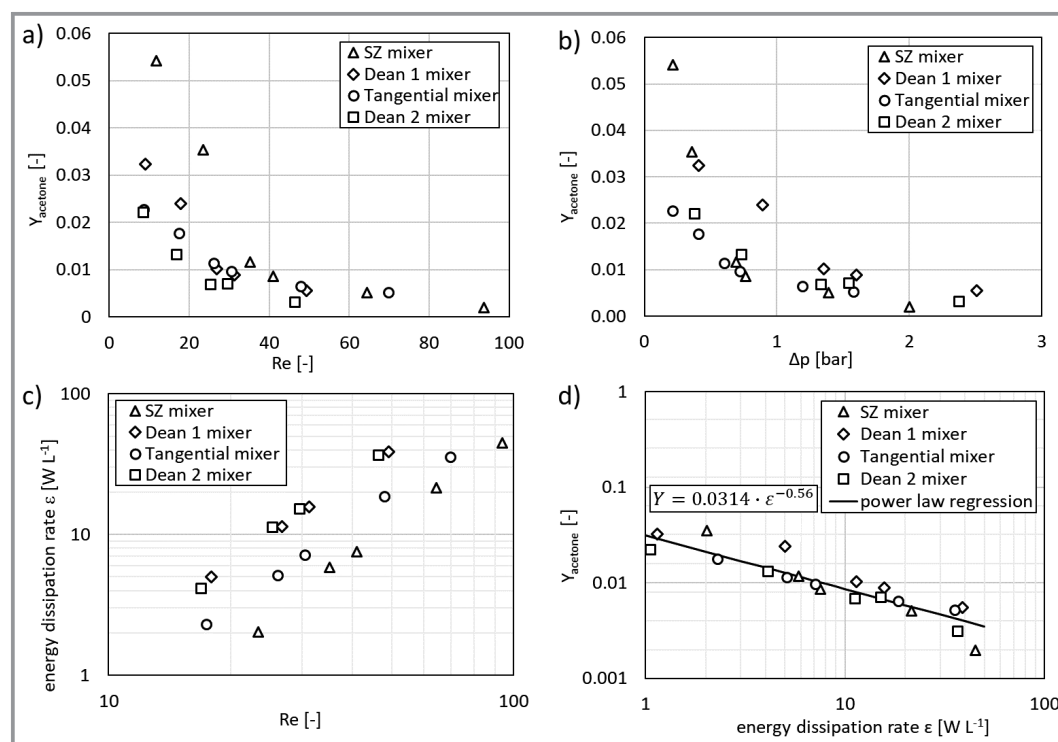


**Figure 4.** a) Obtained yield for acetone over Reynolds number. b) Obtained yield for acetone over pressure drop induced by the mixing structure. c) Energy dissipation rates plotted over Reynolds number. d) Derived yield of acetone over energy dissipation rates with power law regression featuring a coefficient of determination of  $R^2 = 0.85$ .

Holvey et al. [13] measured methanol yield instead of acetone for evaluating the same reaction system and reached comparable methanol yields below 0.1 using a caterpillar mixer with a hydraulic diameter of 600  $\mu\text{m}$ . A comparison of the results of Holvey et al. and the results of this study shows an energy dissipation rate 10 000 times lower. For similar energy dissipation rates between 1 and 50  $\text{W L}^{-1}$ , tangential mixers realized methanol yields between 0.4 and 0.65 [13].

Overall, all four investigated structures display almost similar mixing qualities, leading to the conclusion that the structure has only a minor effect on the mixing quality for the investigated Reynolds number range and all four mixing structures operate at the same mixing time scale.

## 5 Conclusion and Outlook

Four microfluidic devices manufactured by a newly developed reactive etching process were applied on a mixing-sensitive consecutive reaction system. By implementing a test rig including online UV/Vis spectrometry, it was possible to measure the resulting acetone concentration after the mixing structures. By relating the derived yield regarding acetone with the Reynolds number, fast mixing of all investigated microstructures leads to a yield below 1 % for Reynolds numbers between 40 and 80.

Finally, the correlation of the yield regarding acetone with the specific energy dissipation rate indicated similar mixing time scale for all investigated micromixers. In contrast to results found by Holvey et al. [13] for mixers with 10 times larger hydraulic diameters and similar energy dissipation rates between 2 and 40  $\text{W L}^{-1}$ , the evaluated mixing structures of this work show single digit acetone or methanol yields, respectively, for all investigated process parameters.

Reactive ion etching is suitable as a fast and easy manufacturing technique for microfluidic devices in the micrometer range with rectangular channel geometries. This application shows the possibility to manufacture microstructures when they are needed in the lab leading to a fast installation of an experimental setup and accelerated process development.

As an outlook, the manufacturing process needs to be revised and optimized regarding reproducibility of channel depths and roughness. Especially, the photolithography process is to be optimized as inclination angles of the photo resist, affect the aspect ratio and the precise etching of the channel. For further applications, mixing-sensitive nucleophilic additions as lithiations are attractive, since single addition is needed and the multiple addition should be avoided.

The authors thank the Smart Microsystems Institute, TU Dortmund University, for providing the technology of reactive ion etching, photolithography, and fruitful discussions. Open access funding enabled and organized by Projekt DEAL.

## Symbols used

$a$	[-]	aspect ratio
$c$	[ $\text{mol L}^{-1}$ ]	concentration
$d_h$	[m]	hydraulic diameter
$p$	[bar]	pressure
$R_q$	[m]	root mean square roughness
$Re$	[-]	Reynolds number
$T$	[ $^{\circ}\text{C}$ ]	temperature
$V$	[ $\text{m}^3$ ]	volume
$Y$	[-]	yield

## Greek letters

$\varepsilon$	[ $\text{W L}^{-1}$ ]	specific energy dissipation rate
$\tau$	[s]	hydraulic residence time

## Sub- and Superscripts

0	start
mix	mixing

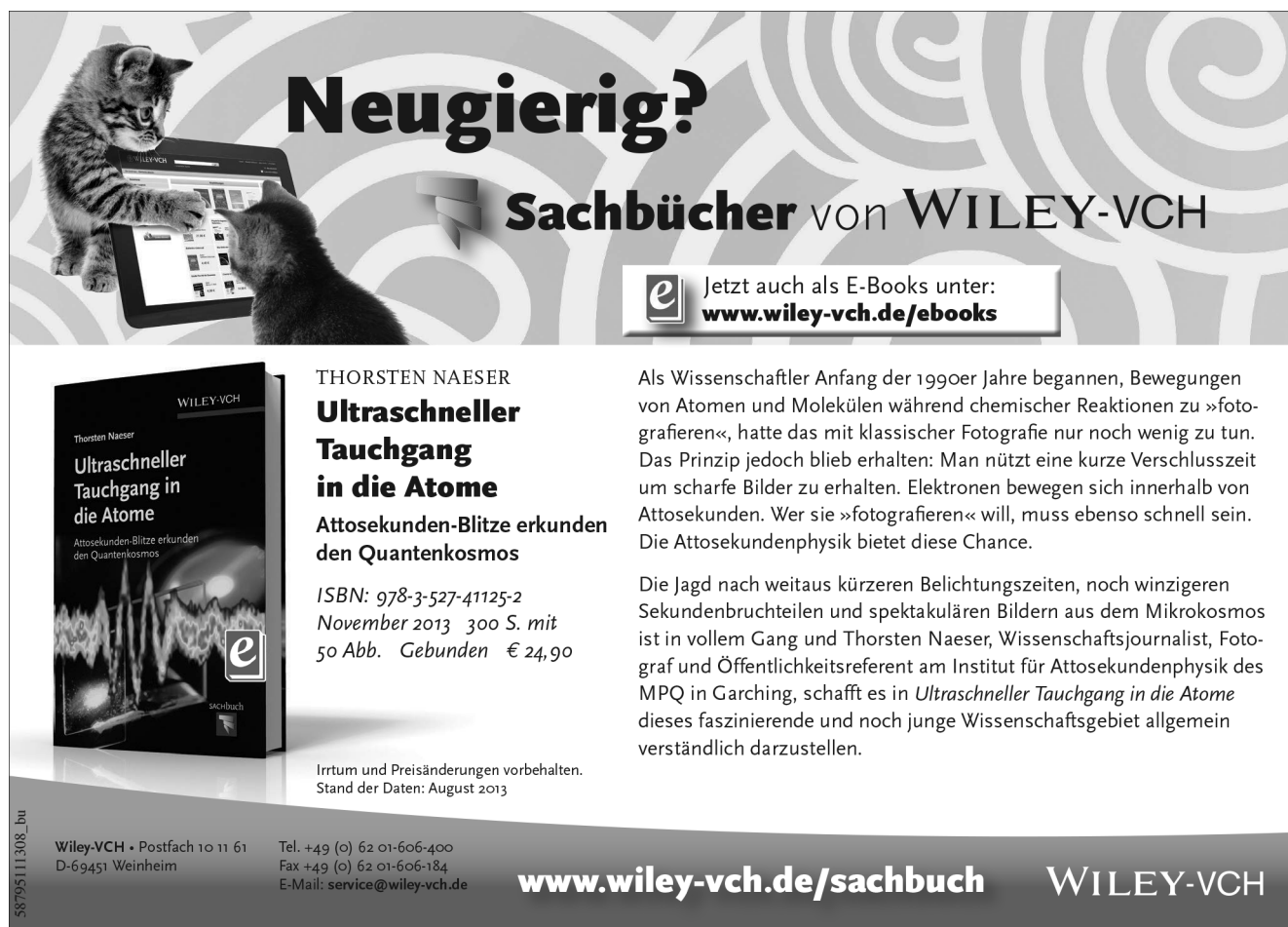
## Abbreviations

DMP	2,2-dimethoxypropane
PI	polyimide

## References

- [1] A. Macchi, P. Plouffe, G. S. Patience, D. M. Roberge, *Can. J. Chem. Eng.* **2019**, *97* (10), 2578–2587. DOI: <https://doi.org/10.1002/cjce.23525>
- [2] X. Zhang, S. Stefanick, F. J. Villani, *Org. Proc. Res. Dev.* **2004**, *8* (3), 455–460. DOI: <https://doi.org/10.1021/op034193x>
- [3] K. F. Jensen, *Chem. Eng. Sci.* **2001**, *56* (2), 293–303. DOI: [https://doi.org/10.1016/S0009-2509\(00\)00230-X](https://doi.org/10.1016/S0009-2509(00)00230-X)
- [4] N. Kockmann, *Proc. Inst. Mech. Eng., Part C* **2008**, *222* (5), 293–303. DOI: <https://doi.org/10.1243/09544062JMES717>
- [5] S. Metz, R. Holzer, P. Renaud, *Lab Chip* **2001**, *1* (1), 29–34. DOI: <https://doi.org/10.1039/B103896F>
- [6] J. Bobers, M. Hesselmann, A.-C. Schneider, J. Zimmermann, N. Kockmann, in *Proc. of the 17th Int. Conf. on Nanochannels, Microchannels, and Minichannels*, American Society of Mechanical Engineers, **2019**. DOI: <https://doi.org/10.1115/ICNMM2019-4208>

- [7] G. Rinke, A. Ewinger, S. Kerschbaum, M. Rinke, *Microfluid. Nanofluid.* **2011**, *10* (1), 145–153. DOI: <https://doi.org/10.1007/s10404-010-0654-8>
- [8] S. Schwolow, J. Hollmann, B. Schenkel, T. Röder, *Org. Proc. Res. Dev.* **2012**, *16* (9), 1513–1522. DOI: <https://doi.org/10.1021/op300107z>
- [9] M. N. Kashid, A. Renken, L. Kiwi-Minsker, *Microstructured Devices for Chemical Processing*, Wiley-VCH, Weinheim **2015**.
- [10] M. A. Ansari, K.-Y. Kim, *AIChE J.* **2009**, *55* (9), 2217–2225. DOI: <https://doi.org/10.1002/aic.11833>
- [11] A. Sudarsan, V. Ugaz, *Proc. Natl. Acad. Sci. U. S. A.* **2006**, *103* (19), 7228–7233. DOI: <https://doi.org/10.1073/pnas.0507976103>
- [12] F. Schönfeld, S. Hardt, *AIChE J.* **2004**, *50* (4), 771–778. DOI: <https://doi.org/10.1002/aic.10071>
- [13] C. P. Holvey, D. M. Roberge, M. Gottsponer, N. Kockmann, A. Macchi, *Chem. Eng. Process.* **2011**, *50* (10), 1069–1075. DOI: <https://doi.org/10.1016/j.cep.2011.05.016>
- [14] A. Tollkötter, A. Sackmann, T. Baldhoff, W. K. Schomburg, N. Kockmann, *Chem. Eng. Technol.* **2015**, *28* (7), 1113–1121. DOI: <https://doi.org/10.1002/ceat.201400522>
- [15] N. Kockmann, *Transport Phenomena in Micro Process Engineering*, 1st ed., Heat and mass transfer, Springer-Verlag, Berlin **2008**.
- [16] L. Falk, J.-M. Commenge, *Chem. Eng. Sci.* **2010**, *65* (1), 405–411. DOI: <https://doi.org/10.1016/j.ces.2009.05.045>
- [17] N. Kockmann, *Chem. Eng. Technol.* **2008**, *31* (8), 1188–1195. DOI: <https://doi.org/10.1002/ceat.200800065>



# Neugierig?

## Sachbücher von WILEY-VCH

Jetzt auch als E-Books unter:  
[www.wiley-vch.de/ebooks](http://www.wiley-vch.de/ebooks)

**THORSTEN NAESER**  
**Ultraschneller Tauchgang in die Atome**  
Attosekunden-Blitze erkunden den Quantenkosmos

ISBN: 978-3-527-41125-2  
November 2013 300 S. mit 50 Abb. Gebunden € 24,90

Irrtum und Preisänderungen vorbehalten.  
Stand der Daten: August 2013

Als Wissenschaftler Anfang der 1990er Jahre begannen, Bewegungen von Atomen und Molekülen während chemischer Reaktionen zu »fotografieren«, hatte das mit klassischer Fotografie nur noch wenig zu tun. Das Prinzip jedoch blieb erhalten: Man nützt eine kurze Verschlusszeit um scharfe Bilder zu erhalten. Elektronen bewegen sich innerhalb von Attosekunden. Wer sie »fotografieren« will, muss ebenso schnell sein. Die Attosekundenphysik bietet diese Chance.

Die Jagd nach weitaus kürzeren Belichtungszeiten, noch winzigeren Sekundenbruchteilen und spektakulären Bildern aus dem Mikrokosmos ist in vollem Gang und Thorsten Naeser, Wissenschaftsjournalist, Fotograf und Öffentlichkeitsreferent am Institut für Attosekundenphysik des MPQ in Garching, schafft es in *Ultraschneller Tauchgang in die Atome* dieses faszinierende und noch junge Wissenschaftsgebiet allgemein verständlich darzustellen.

Wiley-VCH • Postfach 10 11 61  
D-69451 Weinheim  
Tel. +49 (0) 62 01-606-400  
Fax +49 (0) 62 01-606-184  
E-Mail: [service@wiley-vch.de](mailto:service@wiley-vch.de)

[www.wiley-vch.de/sachbuch](http://www.wiley-vch.de/sachbuch) WILEY-VCH